

Water-soluble binder of cellulose acetate butyrate/poly(ethylene glycol) blend for powder injection molding

MIN SOO PARK, JIN KON KIM*

Department of Chemical Engineering and Polymer Research Institute, Electronic and Computer Engineering Divisions, Pohang University of Science and Technology, Pohang, Kyungbuk 790-784, Korea
E-mail: jkkim@postech.ac.kr

SANGHO AHN, HWAN JIN SUNG

Pohang Research Institute of Industrial Science and Technology, Pohang, Kyungbuk 790-784, Korea

A new binder system consisting of cellulose acetate butyrate (CAB) and poly(ethylene glycol) (PEG) with various molecular weights was introduced. CAB and PEGs with various molecular weights had good compatibility. The blends exhibited low enough viscosity to make homogeneous feedstock for the injection molding. Shape maintenance during the extraction by an environmentally favored solvent of water was excellent, and final sintered parts had excellent dimensional stability ($\pm 0.3\%$) and high sintered density over 98%. We also found that injection cycle time was comparable to that of commonly used wax-based feedstock. © 2001 Kluwer Academic Publishers

1. Introduction

Powder injection molding (PIM) processing of metals or ceramics has been currently employed to develop tiny and sophisticated metal or ceramic parts and this is a very economic process compared with a casting and a machining method [1, 2]. It consists of the preparation of a feedstock by the mixing of a binder and metal powders, injection molding of the feedstock into a mold, removal of the binder from the feedstock (debinding), and sintering of the metal or ceramic powders. Among many steps in the PIM, the proper choice of a binder becomes crucial to have better mechanical properties of a feedstock and final product, because a feedstock is usually fragile and brittle due to high metal or ceramic powder content and lower strength of binders. The binder systems are usually composed of polymer mixtures; for instance, (i) backbone material to maintain the shape during the debinding, (ii) low viscosity material to lower the viscosity to make it suitable for injection molding as well as to have good extractability by solvent during the debinding, (iii) and small amount of additives to improve the wettability between binder and powder [3]. Currently, wax-based binders with backbone material of polyethylene or a poly(ethylene-ran-vinyl acetate) have been widely used in the powder injection molding industries [4, 5]. But, in this binder system, in order to extract the wax, one must employ organic solvents such as hexane and heptane, which cause environmental problems. Thus, it is needed to develop

new binder system including a low viscous material that is extracted by an environmentally favored solvent such as water or alcohol. In this study, water-soluble poly(ethylene glycol)s (PEG) with various molecular weights were chosen for this purpose. As a backbone material, cellulose acetate butyrate (CAB) with side-groups substituted by COCH_3 and COC_3H_7 from cellulose was selected. This is because CAB shows (i) good miscibility with PEG, (ii) high glass transition temperature ($T_g = 94^\circ\text{C}$) and (iii) very rigid material required for the shape maintenance during the extraction. Emphasis is placed upon the effect of the molecular weight of PEG on the shape maintenance during the extraction.

2. Experimental

2.1. Materials

CAB with 54 mol% butyrate side group was purchased from Acros Co. and PEGs were kindly supplied by Korea Polyol Co. (Korea). The molecular characteristics of these materials were given in Table I. CAB is an amorphous material with the glass transition temperature of 94°C , measured by DSC (Perkin-Elmer DSC 7 series) at a heating rate of $20^\circ\text{C}/\text{min}$. Two types of stainless steel powders were employed in this study: one was water-atomized 17-4PH (STS, Mitsubishi Steel MFG Co.) with irregular shape and the average particle diameter of $8\ \mu\text{m}$, the other was gas-atomized Osprey (316L STS, Osprey Steel Co.) with round shape and

*Author to whom all correspondence should be addressed.

TABLE I Molecular characteristics of blend components employed in this study

	M_n	PDI	T_g or T_m ($^{\circ}\text{C}$)
CAB	11,000	2.3	$T_g = 94$
PEG-1	1,500	1.15	$T_m = 43$
PEG-2	2,000	1.10	$T_m = 50$
PEG-3	3,350	1.14	$T_m = 54$
PEG-8	8,000	1.16	$T_m = 56$
PEG-15	15,000	1.17	$T_m = 60$

PDI: polydispersity index.

the average particle diameter of $10\ \mu\text{m}$. The chemical compositions of two powders are given in Table II.

2.2. Sample preparation and rheological properties

Binders consisting of CAB/PEGs (35/65 wt/wt) were prepared with a mechanical stirrer at 150°C for 30 min. The feedstock, a mixture of the binder and metallic powder, was first prepared by mixing at 150°C for 1 hr using Kneading Blade Type Mixer (IKAVISC Co.); then it was shaped into a rectangular bar $70.22 \times 7.12 \times 3.57\ \text{mm}$ (L \times W \times T) by using a precision injection-molding machine (Technoplas Co.) with injection pressure of 20 MPa at 130°C and mold temperature of 20°C .

An Advanced Rheometrics Expansion System (ARES) using the dynamic oscillatory mode with parallel plates fixture (25 mm diameter) was used to measure the viscosity of the binder itself. The sample gap was 1.2 mm.

2.3. Synchrotron small angle X-ray scattering

The SAXS measurements with synchrotron radiations were conducted at the 4C1 beam line at the Pohang Light Source (PLS) [6], Korea. The primary beam was monochromatized with double Si(111) crystals at the wavelength of 0.15402 nm (the X-ray photon energy is 7.76 keV) and then it was focused on a detector plane by a bent cylindrical mirror. A one-dimensional position sensitive detector (Diode-Array PSD; Princeton Instruments Inc.; Model ST-120) with the distance of each diode of $25\ \mu\text{m}$ was used. The sample thickness was 1 mm. We subtracted the scattering intensity of an empty cell with two pieces of thin polyimide (Kapton) films from that of samples by taking into account of transmittance of X-rays through the samples. A contribution of thermal diffuse scattering (TDS) arising from the density fluctuations was further subtracted. Here, we approximated that the intensity at the high q region, where the scattering intensity is independent of q , is

identical to the intensity level of TDS. Here, q is the magnitude of the scattering vector, $q = (4\pi/\lambda)\sin(\theta/2)$. Here λ and θ are the wavelength of the X-rays and the scattering angle, respectively. The obtained scattering intensities were not converted to absolute units. The exposure time was 30 s.

2.4. Debinding and sintering

Two steps of debinding of green parts were conducted. The first step is called as the solvent extraction; namely PEG was extracted out of green parts by distilled water at room temperature for 12 h. The second step is referred to as the thermal debinding, where the backbone of CAB was completely removed and pre-sintering of metal powders occurred. Finally the sintering of metal powders was carried out. Thermal debinding and sintering were carried out in a tube-type furnace (Lenton Thermal Design Ltd.) under hydrogen atmosphere using the following thermal histories.

Thermal debinding

$20^{\circ}\text{C} \rightarrow 300^{\circ}\text{C}$ (1 hr) $\rightarrow 500^{\circ}\text{C}$ (1 hr)
 ($3^{\circ}\text{C}/\text{min}$) ($3^{\circ}\text{C}/\text{min}$)
 $\rightarrow 850^{\circ}\text{C}$ (1 hr)
 ($5^{\circ}\text{C}/\text{min}$)

Sintering

$20^{\circ}\text{C} \rightarrow 850^{\circ}\text{C}$ (1 hr) $\rightarrow 1100^{\circ}\text{C}$ (1 hr)
 ($5^{\circ}\text{C}/\text{min}$) ($5^{\circ}\text{C}/\text{min}$)
 $\rightarrow 1350^{\circ}\text{C}$ (1 hr)
 ($5^{\circ}\text{C}/\text{min}$)

3. Results and discussion

3.1. Binder properties

Compatibility between constituents in the binder is essential to prepare a homogeneously mixed feedstock. The powder size employed in the PIM industry is usually several micrometers, although fine submicrometer powder is also used for special cases [7]. This implies that the binder components should have compatibility (or miscibility) within the order of submicrometers. Fig. 1 gives optical micrographs (OM) (Axioplan, Zeiss Co.) of CAB/PEG-1 (35/65 wt/wt) binder system measured at 150°C and 25°C , respectively. It is seen that this blend became transparent at 150°C ; thus this suggests that CAB and PEG-1 are completely miscible at 150°C . We also found that all blend compositions of this blend became transparent. Furthermore, unless the molecular weight (M_w) of PEG is larger than 8000, all blends of CAB/PEGs with various M_w are transparent

TABLE II Chemical compositions of 17-4PH and Osprey powders

Wt%	C	Cr	Ni	Si	Mn	Cu	Mo	Nb	P	S	N	O
17-4PH	0.07	15.99	4.15	0.71	0.28	3.88	–	0.35	0.004	0.006	–	0.49
Osprey	0.002	16.7	11.0	0.46	1.30	0.24	2.19	–	0.034	0.007	0.04	0.15

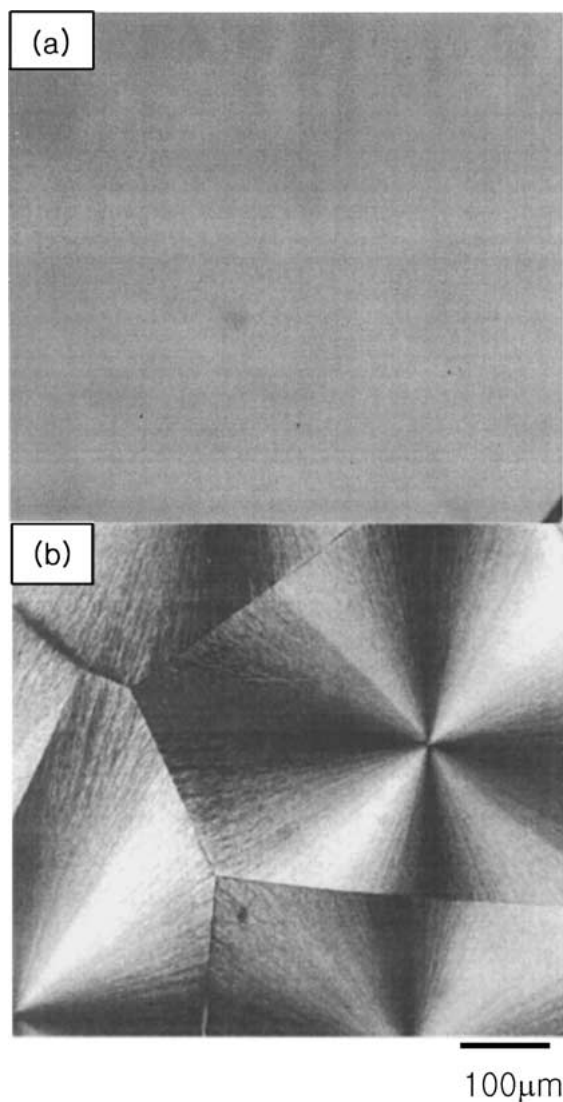


Figure 1 Optical microscopy (OM) images of 35/65 (wt/wt) CAB/PEG-1 blends measured at; (a) molten state of 150°C and (b) crystalline state of 25°C.

in the entire temperature range up to 300°C, above which degradation occurred. However, the mixtures of CAB/PEG showed lower critical solution temperature (LCST) when M_w of PEG was larger than 8000. For instance, the blend CAB/PEG with M_w of 35000 had the LCST of 168°C at the critical composition of 40/60 (wt/wt) CAB/PEG. This indicates that CAB and all PEGs employed in this study do not macrophase-separate during the mixing at 150°C.

Fig. 2 gives complex viscosity (η^*) as a function of frequency for the binders composed of 35/65 (wt/wt) CAB/PEGs with various molecular weights. This binder composition was selected for optimum processing condition for the PIM processing, which allows an easy extraction of the PEG phase without sacrificing shape maintenance during the extraction. It is known that when the viscosity of the binder is below 10 Pa.s, the feedstock including high powder volume does not show any processing problem during injection molding [3]. It is also seen from Fig. 2 that all binders showed Newtonian behavior, η^* of CAB/PEGs binders increases with increasing M_w of PEG, but for all binders it was below 10 Pa.s. Since the viscosity of

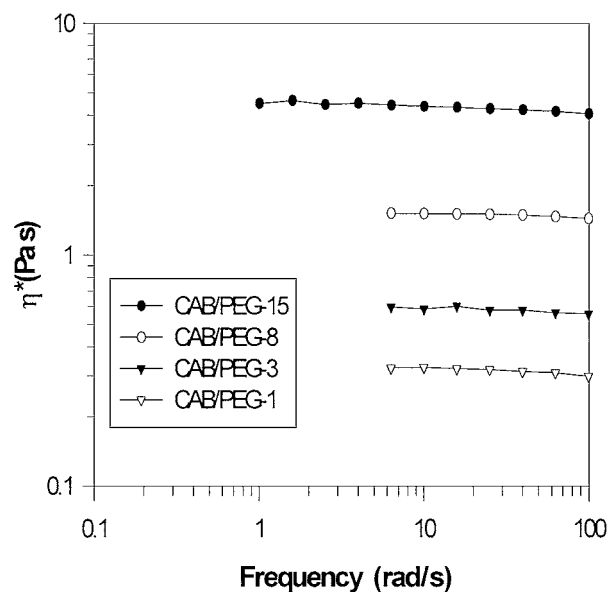


Figure 2 The complex viscosities with frequency measured at 130°C for the blends of CAB/PEGs (35/65 wt/wt).

a suspension with fillers is usually predicted by Equation 1 [8, 9], the viscosity approaches infinity as the volume fraction of the filler becomes the maximum filler loading.

$$\eta = \eta_0 \frac{1}{(1 - \phi/\phi_m)^2} \quad (1)$$

where η is the viscosity of feedstock containing powder and η_0 is the viscosity of the binder itself, and ϕ and ϕ_m are volume fraction of powder and the maximum powder loading, respectively. Since the viscosity of feedstock (or suspension) is proportional to the viscosity of binder itself, one can easily adjust the viscosity of feedstock by selecting different molecular weight of PEG.

3.2. Injection molding and extraction process

An injection molding process was performed for five different feedstocks whose blend compositions are shown in Table III. We found that none of the feedstocks showed any binder separation during the injection molding. The PEG portions in the injection-molded articles (green parts) prepared by all feedstocks were extracted by distilled water at room temperature for 12 h. The shapes of green parts after the extraction

TABLE III Feedstocks consisting 17-4PH powder and CAB/PEG binder systems

	Binder type and composition (wt ratio)	17-4PH powder loading (vol%)
Feedstock 1	CAB/PEG-1 (35/65)	56
Feedstock 2	CAB/PEG-2 (35/65)	56
Feedstock 3	CAB/PEG-3 (35/65)	56
Feedstock 4	CAB/PEG-8 (35/65)	56
Feedstock 5	CAB/PEG-15 (35/65)	56

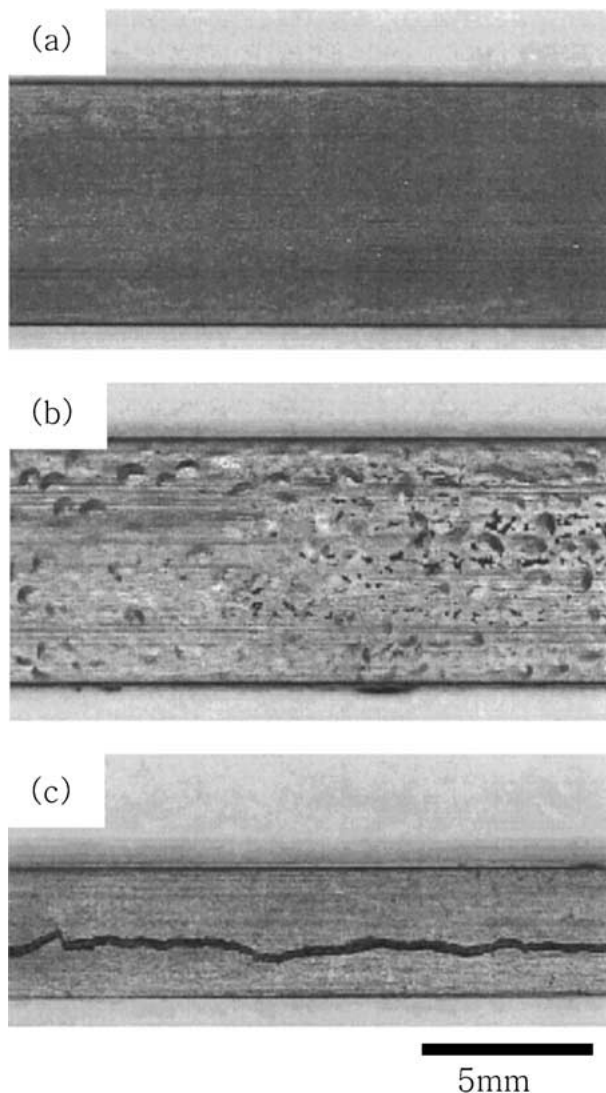


Figure 3 The shapes of injection molded articles (green parts) whose compositions are given in Table III, after the extraction by water at room temperature for 12 hr. (a) Top view of green parts 1 or 2; (b) top view of green part 3; and (c) side view of green part 5.

are illustrated in Fig. 3. It is seen in Fig. 3 that the green parts consisting of CAB/PEG-1 and CAB/PEG-2 binders did not show any cracking during the extraction. But, the green parts consisting of CAB/PEG-3 and CAB/PEG-8 binders exhibited sometimes swellings and cracks at the skin layer, even though most specimens did not show any sign of swelling. Finally, the green parts consisting of CAB/PEG-15 failed to sustain the shapes during the extraction; thus the cracks were clearly observed at the lateral sides.

The failures during the extraction are ascribed to residual stress resulting from a rapid quenching as well as molecular orientation caused by the fast flow that are

usually encountered in the injection molding process [10]. Thus, to investigate in detail the main factor for the failures of green parts during the extraction, we prepared specimens consisting of 17-4PH and CAB/PEGs binders, using compression molding where the residual stress effect can be minimized. After the extraction of PEGs in the specimens by water, we found that the specimens consisting of CAB/PEG-1 and CAB/PEG-2 did not show any failure, while those consisting of CAB/PEG-15 failed to sustain the shape due to the cracks observed at the lateral side of the specimen. These results clearly showed that the different processing conditions (injection vs. compression moldings) did not affect the failures or shape maintenance during the extraction.

It is also noted that the powder loading can affect the capability of the shape maintenance during the extraction (the higher loading, the less possibility of the failures). In order to increase the powder loading, we used gas-atomized Osprey powder with the round shape of average diameter $10\ \mu\text{m}$. In this situation, we could increase the powder loading of Osprey powder up to 70 vol%, which was larger than that (56 vol%) of PH-4PH because of low interparticle friction of the former particle resulting from its round shape. Then, we prepared another feedstock consisting of 70/30 (vol/vol) Osprey/PEG-based binder. The binder compositions in all feedstocks are 35/65 (wt/wt) CAB/PEGs. We employed the same compression molding method and extraction condition as for the case of 17-4PH powders. Table IV gives specimen dimensions (i) before the extraction by water, (ii) right after the extraction of PEG by water, and (iii) after complete drying out in vacuum. It is of interest to note in Table IV that there is no shrinkage in specimens consisting of at least 20 vol% of PEG-1 or PEG-3, even after all PEGs were completely extracted by water. Furthermore, we observed that there was no cracking for these two binder systems after the extraction. However, for green parts consisting of PEG-8 and PEG-15, cracks were found at the edge of the molded parts because of the swelling during the extraction (see the increase in the thickness of the specimen as shown in Table IV).

From these results, we can conclude that the different behavior of the shape maintenance during the extraction between green parts with lower M_w of PEG and those with higher M_w of PEG, mainly resulted from the mechanical properties of the binder itself, even though other factors that we did not mention can influence the shape maintenance. It is known that when the molecular weight of PEG is changed, the crystalline structure of PEG in the binder is also varied [11–13]; thus the mechanical properties of the blends containing PEG are changed. In order to investigate this effect in detail,

TABLE IV Dimensions of compression-molded specimens consisting of 70/30 (vol/vol) Osprey and the binders with 35/65 wt/wt CAB/PEGs measured at various conditions (unit: mm)

Binder type	CAB/PEG-1	CAB/PEG-3	CAB/PEG-8	CAB/PEG-15
After molding	$49.87 \times 24.87 \times 3.16$	$49.87 \times 24.97 \times 3.16$	$49.98 \times 24.95 \times 3.19$	$49.98 \times 24.96 \times 3.15$
After extraction	$49.87 \times 24.87 \times 3.16$	$49.87 \times 24.97 \times 3.16$	$50.02 \times 25.00 \times 3.25$	$50.17 \times 25.07 \times 3.34$
After drying	$49.87 \times 24.87 \times 3.16$	$49.87 \times 24.97 \times 3.16$	$49.94 \times 24.93 \times 3.20$	$49.91 \times 24.93 \times 3.20$

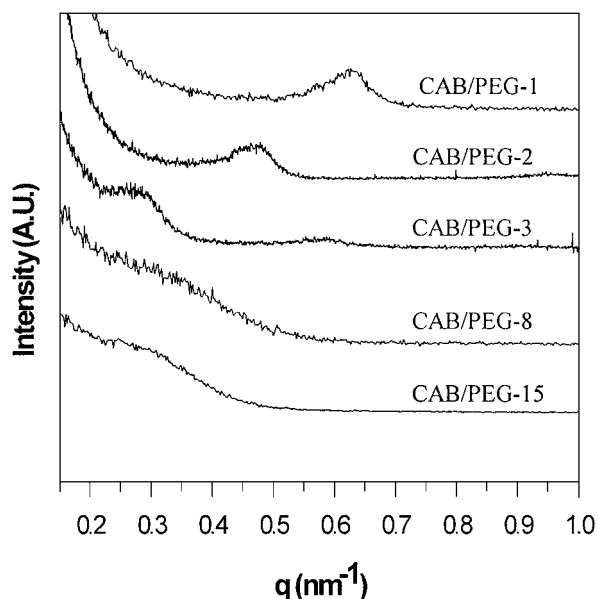


Figure 4 SAXS profiles of CAB/PEGs blends after crystallized at room temperature.

we carried out synchrotron small angle X-ray scattering (SAXS) measurements, and the results are shown in the Fig. 4. It is seen that the domain spacings ($2\pi/q^*$, where q^* is the wavelength with the maximum intensity) of the PEG in both CAB/PEG-1 and CAB/PEG-2 blends were smaller than those in both CAB/PEG-8 and CAB/PEG-15 blends. From the results in ref. [11–13], PEG-1 and PEG-2 have extended chain crystals, while PEG-8 and PEG-15 exhibit folded chain crystals. Interestingly, PEG-3 has two crystal forms; extended chain crystals occurring at a lower q (0.28 nm^{-1}), and 1-folded crystals occurring at a higher q (0.59 nm^{-1}). This is also consistent with results that a PEG with the molecular weight about 3000–4000 exhibits two crystal types [12]. Therefore, one can speculate that the size of crystal of PEG in the binder was related to the shape maintenance during the extraction; the bigger the crystal, the poorer the shape maintenance since a larger area is exposed to the solvent. The details on crystallization kinetics and crystal forms and their dependence upon molecular weight of PEG were discussed elsewhere [14].

3.3. Thermal debinding and sintering

Fig. 5 gives the weight loss with temperature for CAB and PEG-8 in two different environments. It is shown that PEG-8 did not have any residue at temperatures higher than 420°C . But, CAB was not completely pyrolyzed even at 600°C under nitrogen atmosphere, while this completely disappeared at 600°C under air environment, which implied that CAB/PEGs binder can be completely removed under air atmosphere. However, the use of air atmosphere is not good for metal powder due to oxidization of the metal. Thus, hydrogen atmosphere was employed for the thermal debinding of green parts with metal powders. After almost all PEGs in 56/44 (vol/vol) 17-4PH/the binder with 35/65 (wt/wt) CAB/PEG-2 blend were extracted by water, the resid-

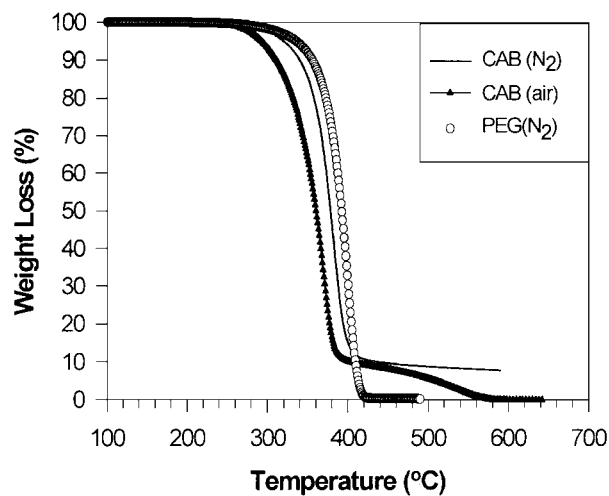


Figure 5 TGA thermograms of CAB and PEG at a heating rate of $20^\circ\text{C}/\text{min}$ under air and nitrogen atmospheres.

ual binder component in the specimens was thermally debinded under hydrogen atmosphere using the thermal histories mentioned in the experimental section. After finishing all thermal histories, residual carbon and oxygen content were measured and are shown in Table V. The original C and O content of 17-4PH powder itself was also added. It is seen that the carbon residue resulted from the binder was slightly increased after thermal debinding, but the oxidation of metal did not occur. Even though a small increase in the carbon after thermal debinding was observed, this carbon residue was further reduced during the sintering process.

The dimensions and densities were measured after the parts were sintered, and are given in Table VI. It is seen that the dimensional standard deviation was less than a commercially allowed tolerance ($\pm 0.3\%$). Furthermore, the final density was more than 98%, which is greater than the commercially required value of 95%. The final sintered part and green part prepared from feedstock 2 are shown in Fig. 6, from which one notes that the sintered part was reduced uniformly from the original size of green part and shows a typical metal gloss. Finally, we considered the cycle time for injection

TABLE V Carbon and oxygen contents of original 17-4PH powder and thermally debinded 17-4PH powder

Wt%	Original powder	After pyrolysis
Carbon	0.07	0.12
Oxygen	0.49	0.49

TABLE VI Dimensions and densities of final parts fabricated by the feedstock 2

	Dimension	Standard deviation	Sintered density ^a
Feedstock 2	L	58.495 ± 0.005	$\pm 0.009\%$
	W	$5.830 \pm .0004$	$\pm 0.007\%$
	T	2.905 ± 0.005	$\pm 0.17\%$

^aSintered density: measured density divided by the density of 17-4PH metal ($7.7 \text{ g}/\text{cm}^3$).

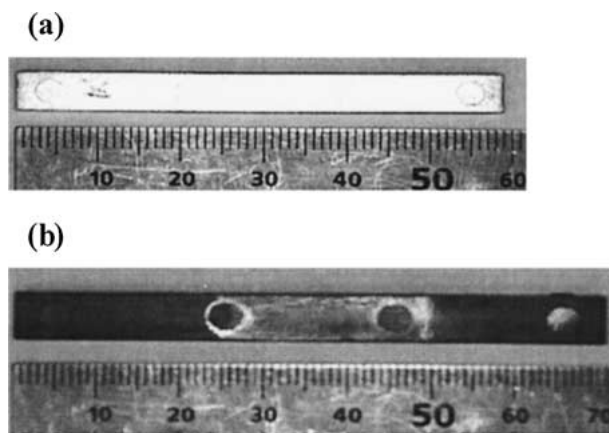


Figure 6 The shapes of (a) the article after sintering and (b) green part prepared by feedstock 2 in Table III.

molding; the shorter, the more economic. The cycle time for feedstock with PEG-1 was 2 min, which is longer than that of a commercially available wax-based binder (~ 1 min). This is due to slow crystallization of PEG-1 because of its very low T_m (43°C), not much higher than the mold temperature (20°C). But as M_w of PEG increased, the injection molding cycle for PEG-2, PEG-3, and PEG-8 could be performed within ~ 1 min. Therefore, it is concluded that the CAB/PEG binder system can be used in industry.

4. Conclusions

We introduced a new binder system consisting of CAB/PEGs blends that is environmentally favorable and excellent in ensuring the dimensional stability in PIM. CAB and PEGs had good compatibility and the blend showed viscosity low enough to fabricate homogeneous feedstock during injection molding. The capability for the shape maintenance during the extraction depended on the PEG molecular weights. The binder systems consisting of CAB and low molecular weight PEGs exhibited excellent shape maintenance. However, as the molecular weight of PEG was increased, CAB/PEG binder failed to maintain the shape during the extraction. The final dimensional stability was ex-

cellent (within $\pm 0.3\%$) and the sintered density was over 98%. When considering many advantages over a commercially employed wax-based binder such as excellent dimensional stability, easier processing conditions for injection molding and debinding, and higher sintered density, CAB/PEGs binder systems would be very competitive and have the potential to be commercially employed.

Acknowledgement

This work was supported by Korea Institute of Industrial Technology Evaluation and Planning. Synchrotron SAXS experiments were performed at the PLS (3C2 and 4C1 beam lines) in Korea, which was supported by MOST and POSCO.

References

1. R. M. GERMAN, "Powder Injection Molding" (Metal Powder Industries Federation, Princeton, NJ, 1990) p. 3.
2. B. CARPENTER, PhD thesis, Rensselaer Polytechnic Institute, NY, 1988, p. 1.
3. C. I. CHUNG, B. O. RHEE, M. Y. CAO and C. X. LIU, "Advances in Powder Technology," Vol. 1 (Metal Powder Industries Federation, Princeton, NJ, 1989) p. 67.
4. J. K. KIM and B. KIM, *J. Polym. Sci.: Polym. Phys. Ed.* **37** (1999) 1991.
5. *Idem.*, *J. Japan Soc. Powder and Powder Mett.* **46** (1999) 823.
6. B. J. PARK, S. Y. RAH, Y. J. PARK and K. B. LEE, *Rev. Sci. Instrum.* **66** (1995) 1722.
7. R. M. GERMAN, "Injection Molding of Metals and Ceramics" (Metal Powder Industries Federation, Princeton, NJ, 1997) p. 55.
8. T. KITANO, *Rheol. Acta* **17** (1978) 149.
9. *Idem.*, *ibid.* (1981) 206.
10. K. E. HRDINA and J. W. HALLORAN, *J. Mater. Sci.* **33** (1998) 2805.
11. J. BLDRIAN and M. HORKY, *Polymer* **40** (1999) 439.
12. S. Z. D. CHENG, A. ZHANG, J. S. BARLEY, J. CHEN, A. HABENSCHUSS and P. R. ZSCHACK, *Macromolecules* **24** (1991) 3937.
13. *Idem.*, *ibid.* **25** (1992) 1453.
14. M. S. PARK, MS thesis, Pohang University of Science and Technology, 2001.

Received 6 June
and accepted 20 August 2001